INSTRUMENTAL CORRECTION OF THE IMAGES DISTORTED BY A SCATTERING MEDIUM

A.N. Alekseev, V.V. Belov, B.D. Borisov, and N.V. Molchunov

Institute of Atmospheric Optics,
Siberian Branch of the Russian Academy of Sciences, Tomsk
Received May 14, 1992

Results of application of the instrumental correction of the images distorted by the scattering media are discussed. Correction is based on suppression of scattered and amplification of unscattered components of the signal. Results of laboratory experiments on observation of the objects through the scattering media using the specially developed electronic unit of image correction are presented. Results of instrumental correction and numerical filtering of the images distorted by a scattering medium are compared.

The problem of restoring the images distorted by the dense scattering media is the central problem of the theory of vision. Several approaches to its solution are possible. In the first case the solution is sought with the use of the algorithms of numerical filtering, in the second case the hardware is used for the correction of the image signal, and in the third case the special instrumental–program complexes of image restoring are developed.[1–3]

The problems of application of the effective algorithms of numerical filtering of the images distorted by the dispersed media were studied in Refs. 4–6. In the present paper one of the possible simple procedures for the instrumental correction of the images is considered and some results of its application to observation of the self–glowing objects in a laboratory experiment performed in the Institute of Atmospheric Optics of the Siberian Branch of the Russian Academy of Sciences are discussed.

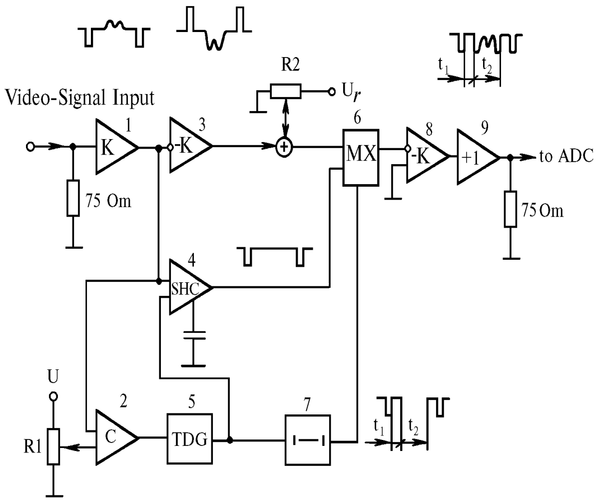

FIG. 1.

With the help of an electronic device designed in the given circuit the shift and referencing of the level of black TV–signal from a TV–camera are performed depending on the level of the background component of the video signal. A block diagram of this device is shown in Fig. 1. It comprises the input amplifier *1*, the comparator *2*, the amplifier–inverter *3*, the sample–and–hold circuit (SHC) *4*, the time–delay generator *5* triggering the SHC and the controllable line sector, the multiplexer *6*, the time–delay generator of the controllable sector *7*, the amplifier–inverter *8*, and the output amplifier *9*.

The circuit of referencing and shift operates in the following way. The signal from the video–camera output is fed to the input amplifier *1* and further to the comparator *2*, the amplifier–inverter *3*, and the SHC *4*. The amplitude of the synchronizing pulses is fixed with the help of the comparator and precise temporal referencing of triggering of the SHC and of the time–delay generator of the controllable line sector is performed. The SHC stores the value of the input signal, i.e., the level of background is fed to one of the inputs of the multiplexer *6*. The amplified video signal is fed to the other input of the multiplexer through the summator which shifts the level of the signal by controlling the reference voltage U_r. With the help of signals formed by the time–delay circuit *7* over the period of recording of one line the multiplexer alternately passes the level of background from the SHC and the video signal at the input of the inverting amplifier *8* performing its inset in the selected section of the line after the time t_1 for the time t_2. The video signal formed in such a way is fed to the input of a 8–bit ADC through the power amplifier *9* and then with the help of the system of image input and processing[7] the frame is recorded on a hard disk. As a result of such a preprocessing we succeeded in using more completely the number of bits of the ADC (the least significant bits are switched on the valid signal rather than on the background component) and thereby in extending the dynamic range of the recorded signal. The circuit makes it possible to use the ADC with lesser numbers of bits and, consequently, significantly simplifies and makes lower in cost the entire channel of image recording and storage.

The device was tested in the special laboratory experiment. Its diagram is shown in Fig. 2.

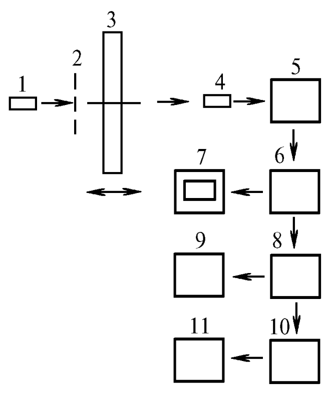

FIG. 2.

The light source *1* with the help of the mask *2* forms the initial object, which is recorded by the TV–system through the cell *3* filled with the model scattering medium. The optical density of the medium is determined by variable concentration of milk dissolved in distilled water. The type of opto–geometric situation of observation[8,9] is modeled by moving the cell along the optical axis.

The distorted image with the help of the TV–camera *4* is transformed into the video signal, which is fed to the ADC of the video processor *6* through the circuit of referencing and shift *5*. From the video processor memory the digitized image with the help of the controlling microcomputer *8* is stored on the disk *9*. For processing of large amount of information, the image is translated with the help of the adapter *10* of the local area network to the high–speed computer *11* of the ES–1066 or IBM/PC–AT386 series. The visual image control is performed by the monitor *7*.

Figure 3 shows the initial object representing three bright triangles with a dark spot in the central part. The raster size is 128×128 pixels. The step of spatial quantization is 0.32 mm/pixel. In order to decrease the noise component of the signal, the image was averaged over 32 frames. Numbers 0, 1, and 2 denote the points used for calculation of the contrast coefficients

$$K1,2 = \frac{E(x_0, y_0) - E(x_{1,2}, y_{1,2})}{E(x_0, y_0) + E(x_{1,2}, y_{1,2})},$$

where $E(x, y)$ is the image amplitude in the selected point of the raster.

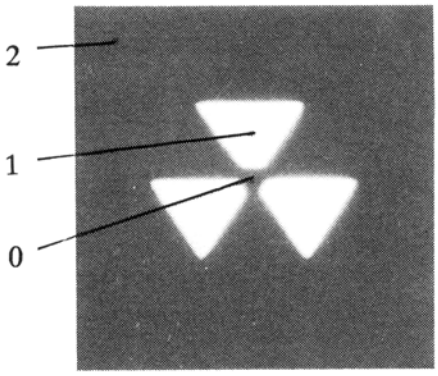

FIG. 3.

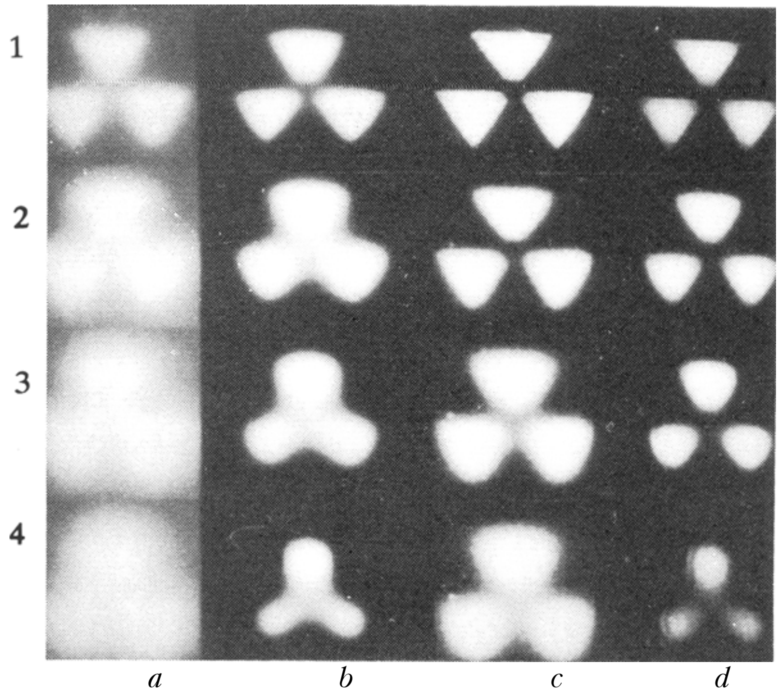

FIG. 4.

Figure 4*a* shows the experimental images recorded in the opto–geometric situation of the first type (the layer of increased turbidity is adjacent to the object) with the scattering medium of different optical thickness. Numbers 1–4 on the left margin of Fig. 4*a* correspond to τ = 3.11, 5.17, 7.41, and 10.03. The letters on the bottom margin of the figure correspond to: images obtained using the unit of fixation and shift of the background component of signal (*b*), the results of numerical filtering of the images (*a*) by Tikhonov's technique[10,11] (*c*), and the results of Tikhonov's filtering of the images (*d*).

Figure 5 shows the images in the opto–geometric situation of the second type (the layer of increased turbidity lying between the object and observer). The numbers and letters on the margins of Fig. 5 correspond to those in Fig. 4 except τ = 10.03. Restoration by Tikhonov's technique in both cases was performed using the point spread function (PSF) calculated in the numerical experiment by the Monte Carlo method.

Figure 6 shows the images obtained in the opto–geometric situation of the third type (the layer of increased turbidity is adjacent to the observer).

The values of the single–point characteristics of the image quality for the given images are listed in Tables I–IV, in which the numbers 1, 2, and 3 denote the types of opto–geometric situations.

1
2
3
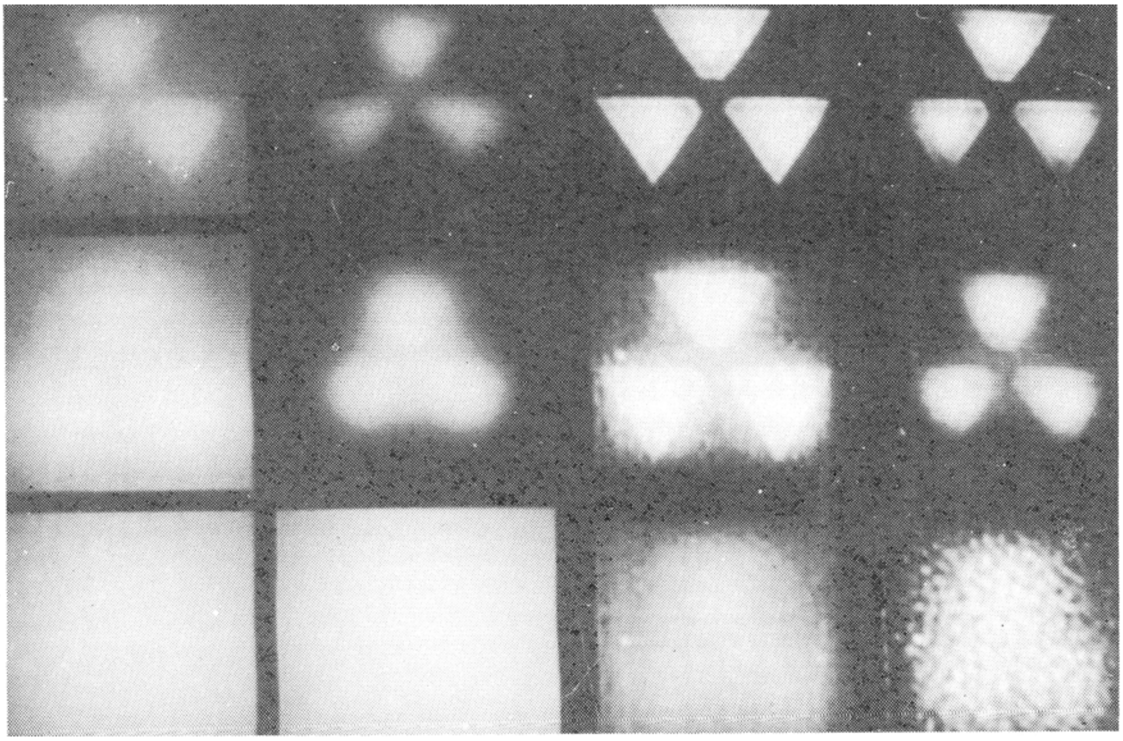
a b c d

FIG. 5.

1
2
3
4
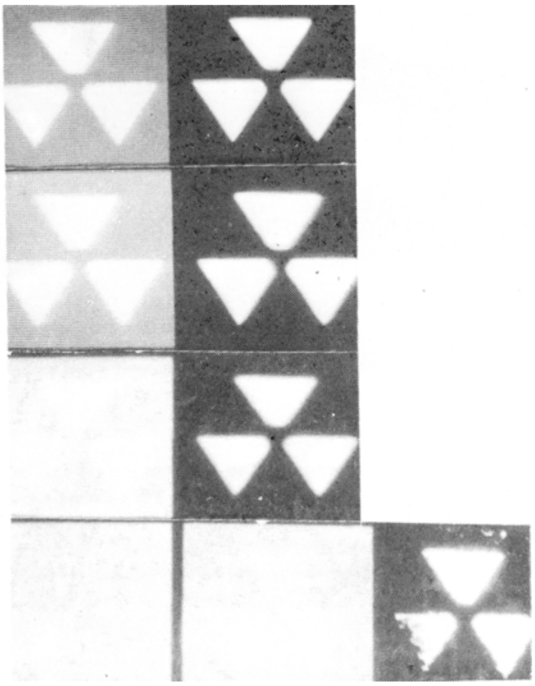
a b c

FIG. 6.

TABLE I. $\tau = 3.11$.

	Distorted image (*a*)			Instrumental correction (*b*)			Restoration by Tikhonov's technique (*c*)		
	Norma-lized rms error	*K*1	*K*2	Norma-lized rms error	*K*1	*K*2	Norma-lized rms error	*K*1	*K*2
1	66.3	0.22	0.54	47.2	0.48	1.00	43.1	0.77	0.69
2	74.7	0.09	0.49	64.4	0.31	1.00	61.6	0.47	0.47
3	58.6	0.47	0.48	50.7	1.00	0.98	–	–	–

TABLE II. $\tau = 5.17$.

	Distorted image (*a*)			Instrumental correction (*b*)			Restoration by Tikhonov's technique (*c*)		
	Norma-lized rms error	*K*1	*K*2	Norma-lized rms error	*K*1	*K*2	Norma-lized rms error	*K*1	*K*2
1	71.0	0.14	0.56	49.8	0.33	1.00	46.1	0.86	0.84
2	85.0	–0.03	0.41	69.8	0.02	–1.0	54.0	0.71	0.74
3	63.8	0.39	0.41	26.2	1.00	1.00	–	–	–

TABLE III. $\tau = 7.41$.

	Distorted image (*a*)			Instrumental correction (*b*)			Restoration by Tikhonov's technique (*c*)		
	Normalized rms error	*K*1	*K*2	Normalized rms error	*K*1	*K*2	Normalized rms error	*K*1	*K*2
1	74.8	0.06	0.53	63.6	0.21	1.00	49.8	0.78	0.75
2	90.5	–0.05	0.28	94.7	–0.08	0.69	61.5	0.76	0.79
3	85.3	0.11	0.13	52.0	0.97	0.98	–	–	–

TABLE IV. $\tau = 10.03$.

	Distorted image (*a*)			Instrumental correction (*b*)			Restoration by Tikhonov's technique (*c*)		
	Normalized rms error	*K*1	*K*2	Normalized rms error	*K*1	*K*2	Normalized rms error	*K*1	*K*2
1	78.9	0.04	0.50	79.1	0.06	1.00	61.4	0.37	0.46
2	–	–	–	–	–	–	–	–	–
3	86.6	0.01	0.02	83.1	0.09	0.07	–	–	–

Analysis of the data obtained enables us to make several conclusions. Inserting the device for contrast correction in the recording channel positively affects the formed image in all the opto–geometric situations of observation. Thus, in the situations of the first type the improvement of the quality characteristics can be seen for the optical thicknesses of the scattering layer up to 10. In the situations of the second type the positive result can be noted for the layers at $\tau < 5$. The most pronounced effect, as expected, is obtained in the opto–geometric situation of the third type. For $\tau = 7.41$ and less we succeeded in complete suppressing the background illumination and increasing the contrast coefficient practically up to unity. For $\tau = 7.41$ we succeeded in amplifying and recording the image of the object being indistinguishable against the background (the contrast coefficient is $K1 = 0.01$). Application of such simple procedures as subtracting the average level of the background illumination and scaling of the amplitude in the range 0–255 to the obtained amplified image enables us to restore the structure and intensity of the initial object (Fig. 6*c*).

Filtering of the distorted images by Tikhonov's technique using the PSF calculated by the Monte Carlo method yields the following results. In the situations of the first type the improvement of the system resolution is found to occur for the optical thicknesses up to 10, whereas the shape of the object is restored satisfactorily for $\tau < 7$. In the situations of the second type the positive effect of the numerical filtering can be seen for $\tau < 5$. It should be noted that filtering of images subjected to the *a priori* instrumental correction of the contrast results in no additional improvement of the quality characteristics. In the situations of the third type the use of the numerical filtering, which performs frequency correction of the signal, is meaningless, because in these cases only the loss of the image contrast occurs without changing its frequency characteristics.

REFERENCES

1. H.C. Andrews and L.H. Enloe, Proc. IEEE (special issue) **60**, No. 7 (1972).
2. G.I. Vasilenko and A.M. Taratorin, *Restoration of Images* (Radio i Svyaz', Moscow, 1986), 302 pp.
3. R.H.T. Bates and M. McDonnell, *Image Restoration and Reconstruction (Clarendon Press, Oxford, 1986)*.
4. V.T. Kalayda, N.V. Molchunov, and S.V. Sapozhnikov, Atm. Opt. **2**, No. 6, 539–544 (1989).
5. V.V. Belov and N.V. Molchunov, in: *Abstracts of Reports at the International Conference on Image Processing and Studies by Remote Sensing Methods (IPSRSM)*, Novosibirsk, 35–36 (1990).
6. V.V. Belov, B.D. Borisov, and N.V. Molchunov, Atm. Opt. **4**, No. 8, 593–598 (1991).
7. V.I. Zhuravlev, S.L. Shinkevich, V.A. Gridnev, et al., in: *Problem–Oriented Measuring–Calculational Complexes* (Nauka, Novosibirsk, 1986), pp. 58–62.
8. V.V. Belov, B.D. Borisov, and I.Yu. Makushkina, Opt. Atm. **1**, No. 2, 18–24 (1988).
9. V.V. Belov, Atm. Opt. **2**, No. 8, 649–660 (1989).
10. A.N. Tikhonov and V.Ya. Arsenin, *Methods of Solution of the Ill–Posed Problems* (Nauka, Moscow, 1979), 285 pp.
11. A.N. Tikhonov, A.V. Goncharskii, V.V. Stepanov, and A.G. Yagola, *Numerical Methods of Solving the Ill–Posed Problems* (Nauka, Moscow, 1990), 230 pp.